Fast and efficient computation of high-order Tchebichef polynomials

Sadiq H. Abdulhussain*[1] | Basheera M. Mahmmod[1] | Thar Baker[2] | Dhiya Al-Jumeily[3]

[1]Department of Computer Engineering, University of Baghdad, Baghdad, Iraq
[2]Department of Computer Science, University of Sharjah, Sharjah, UAE
[3]Department of Computer Science, Liverpool John Moores University, Liverpool, United Kingdom

Correspondence
*Sadiq H. Abdulhussain, Department of Computer Engineering, University of Baghdad, Baghdad, 10071, Iraq. Email: sadiqhabeeb@coeng.uobaghdad.edu.iq

Summary

Discrete Tchebichef polynomials (DTPs) and their moments are effectively utilized in different fields such as video and image coding due to their remarkable performance. However, when the moments order becomes large (high), DTPs prone to exhibit numerical instabilities. In this paper, a computationally efficient and numerically stable recurrence algorithm is proposed for high order. The proposed algorithm is based on combining two recurrence algorithms. In addition, an adaptive threshold is used to stabilize the generation of the DTP coefficients. The designed algorithm can generate the DTP coefficients for high order and large signal size. To evaluate the performance of the proposed algorithm, a comparison study is performed with state-of-the-art algorithms in terms of computational cost and capability of generating DTPs with large size and high order. The results show that the proposed algorithm has a remarkable low computation cost and numerically stable compared to other algorithms. The improvement shows that the computation of the polynomial for a limited order is 27x times faster than the efficient algorithm.

KEYWORDS:
Discrete Tchebichef Polynomials, Tchebichef Moments, Propagation Error, Compression, Computation Cost

1 | INTRODUCTION

Moments and their variants have been extensively utilized in signal processing and computer vision applications. Different types of moments have been introduced, namely geometric moments, rotational moments, continuous moments, and discrete orthogonal moments (DOMs)[1]. DOMs are scalar quantities, and they are determined by projecting a signal on the orthogonal polynomial basis without the need for coordinate transformation and continuous integration[2]. They are utilized to represent signals due to their representation ability of signals without information redundancy, energy compaction, and spectral resolution[1].

DOMs are based on orthogonal polynomial basis; therefore, different sets of discrete orthogonal polynomials (DOPs) are presented and developed such as discrete Hahn polynomials[1,3], discrete Krawtchouk polynomials[4], discrete Charlier polynomials[5], and discrete Tchebichef polynomials (DTPs)[6].

Literature have shown that DOMs, which are employing DOPs, are utilized in many applications such as: Face recognition[7], image compression[8], image dithering[9], shot boundary detection[10], speech enhancement[11,12], cough detection[13], and steganography[14].

In addition, video coding (compression) is significantly involved in the application of video transmission. Generally, coding is divided into two types, lossy and lossless[15]. In lossy coding, the information integrity is degraded while high compression is

obtained. On the other hand, in lossless coding, the integrity of information is preserved during the coding processes (encoding and decoding)[15]. Among other transforms, Discrete Tchebichef Transform (DTT) shows remarkable compression ratio because Discrete Tchebichef Moments (DTMs) show a remarkable energy compaction and data decorrelation than other DOPs[2,16,17]. DTPs are generally a two-dimensional array with three parameters which are: 1) the size of the array $N \times N$, 2) the parameter which represents the polynomial order (n), and 3) the parameter which represents the signal index (x). Discrete Tchebichef polynomial coefficients (DTPCs), are defined in terms of hypergeometric series and gamma functions; however, generating the DTPCs will be computationally expensive and numerically unstable. Therefore, DTPCs are recursively computed using three-term recurrence relations. Different recurrence relations have been presented in the literature to solve the issue of DTPCs computation cost.

The first recurrence algorithm was presented by Mukundan et al.[6]. The DTPCs are computed based on the n-direction recurrence algorithm. In this algorithm, the polynomial coefficients at the nth order for each coefficient of the xth index are computed by employing the coefficients at the orders $n-1$ and $n-2$. This algorithm can generate DTPCs for signal with small sizes.

This problem occurs when computing the high order DTPCs, the numerical propagation error increases as the algorithm estimates the coefficients values[18].To address this issue, an x-direction recurrence algorithm was proposed to compute the DTPCs for high polynomial orders. In this algorithm, the DTPCs at the xth index for each coefficient of the nth order are computed by considering the coefficients values at the indices $x-1$ and $x-2$. Although this algorithm increases the polynomial order, it is unable to estimate the DTPCs for high polynomial orders. This is because the values of the $x-1$ and $x-2$ become zeros at high orders; thus, the estimated values of the DTPCs at the xth index become zero.

A new algorithm is presented by Abdulhussain et al.[19] to tackle the problem of the two previous algorithms. The algorithm is designed by integrating both the n- and x-direction recurrence algorithms. This algorithm can estimate the DTPCs for high polynomial orders; however, the orthogonality of the DTP is inaccurate due to numerical approximation.

Recently, an algorithm is proposed by Camacho-Bello and Rivera-Lopez[20] to correct the orthogonality of the DTP using Gram-Schmidt process on the n-direction recurrence algorithm. Although this algorithm stabilizes the orthogonality condition, the computation cost is very high as well as the DTPCs values satisfy the orthogonality condition but they are not accurate, i.e. the values are inaccurately estimated. In addition, the algorithm in[20] is considered computationally complex because of employing Gram-Schmidt process which requires several nested loops.

From previous discussion, the state-of-the-art algorithms presented in[19,20] tried to generate DTPs for large signal size with high polynomial order. However, these algorithms were unable to reduce numerical instability and distortion when the signal size increases or shows a very high computational cost. In other words, these algorithms were unable to generate DTPs with high polynomial order and numerically stable.

Our contribution is two fold. First, we design an algorithm to generate DTPs with large signal size for high polynomial order as well as numerically stable and capable of satisfying the orthogonality condition. Second, the proposed algorithm is based on combining two recurrence algorithms with an adaptive threshold is used to stabilize the generation of the DTPCs. The adaptive threshold is used to investigate the occurrence of the first unstable DTPC value at the nth order.

This paper is organized as follow: Section 2 presents the Tchebichef functions and moments. In Section 3, recurrence relations are discussed. In Section 4, the design of the proposed algorithm is presented. In Section 5, experimental analysis is performed. Finally, the conclusion is presented in Section 6.

2 | PRELIMINARIES

In this section, the DTPs' definitions are given. Then, the computation of Tchebichef Moments (TMs) is presented.

2.1 | The Orthogonal Discrete Tchebichef functions

The nth order of the DTPs ($T_n(x, N)$) in terms of hypergeometric series is given by[6]:

$$T_n(x) = \frac{(1-N)_n}{\sqrt{(2n)!\binom{N+n}{2n+1}}}\, {}_3F_2(-n, -x, 1+n; 1, 1-N; 1)$$
$$n, x = 0, 1, 2, \ldots, N-1; \text{ and } N > 0 \tag{1}$$

where $(\cdot)_k$ is the Pochhammer symbol[21], $\binom{a}{b}$ is the binomial coefficients, and ${}_3F_2(.)$ represents the hypergeometric functions and it is described by a hypergeometric series:

$$ {}_3F_2(-n,-x,1+n;1,1-N;1) = \sum_{k=0}^{\infty} \frac{(-n)_k(-x)_k(1+n)_k}{(1)_k(1-N)_k k!} \tag{2} $$

The set of DTPs functions meets the orthogonality conditions[6]:

$$ \sum_{n=0}^{N-1} t_n(x)t_m(x) = \delta_{mn} = \begin{cases} 1, & n = m \\ 0, & n \neq m \end{cases} \tag{3} $$

where δ_{nm} is known as Kronecher delta.

2.2 | Tchebichef Moments

The TMs set are scalar quantities which are efficient and superior data descriptor[22]. TMs are effectively employed in signal processing and computer vision due to their ability to characterize signals without information redundancy[23]. Generally, The signal information is observed by the lower-order moments. While the signal details is acquired by high-order moments[11]. Basis functions of orthogonal polynomials (OPs) can be used as an approximate solution for differential equations[24].

The TMs ($\mathcal{M}_n$) of a one dimensional signal, $f(x)$, with a length of N samples and maximum moment order Ord are defined as[19]:

$$ \begin{gathered} \mathcal{M}_n = \sum_{x=0}^{Ord} T_n(x)\, f(x), \\ n = 0, 1, \ldots, M \ \text{ and } \ 0 \leqslant Ord \leqslant N-1 \end{gathered} \tag{4} $$

The signal $f(x)$ can be reconstructed from the Tchebichef moment domain as follows:

$$ \begin{gathered} \hat{f}(x) \cong \sum_{n=0}^{Ord-1} \mathcal{M}_n\, T_n(x), \\ x = 0, 1, \ldots, N-1 \ \text{ and } \ 0 \leqslant Ord \leqslant N-1 \end{gathered} \tag{5} $$

where $\hat{f}(x)$ is the reconstructed version of $f(x)$. To represent a two dimensional signal $f(x, y)$ of size $N \times N$ in the Tchebichef moment domain, the TMs $\mathcal{M}_{nm}$ is defined as:

$$ \begin{gathered} \mathcal{M}_{nm} = \sum_{x=0}^{Ord} \sum_{y=0}^{Ord} T_n(x)\, T_m(y)\, f(x,y), \\ n, m = 0, 1, \ldots, Ord \end{gathered} \tag{6} $$

To reconstruct the 2D signal from the Tchebichef moment domain, the inverse formula is used as follows:

$$ \begin{gathered} \hat{f}(x,y) \cong \sum_{n=0}^{Ord-1} \sum_{m=0}^{Ord-1} \mathcal{M}_{nm}\, T_n(x)\, T_m(y), \\ x, y = 0, 1, \ldots, N-1 \end{gathered} \tag{7} $$

where $\hat{f}(x, y)$ is the reconstructed version of $f(x, y)$.

3 | RECURRENCE RELATIONS

The DTPCs are defined in terms of hypergeometric series (Equation (1)) and consequently the computation cost is considered high and numerical instability will occur[20]. Therefore, the three-term recurrence algorithms (TTRA) are employed to reduce the computational complexity and the instability in the generation of the DTPCs values[2].

In the following subsections, the existing recurrence algorithms are outlined. These algorithms include: the recurrence algorithm in the n-direction[6], the recurrence algorithm in the x-direction[18], the recurrence relation proposed by Camacho-Bello and Rivera-Lopez[20], and Abdulhussain et al.[19] are investigated.

3.1 | Recurrence Algorithm in the *n*-direction (RAND)

The first TTRA was proposed by Mukundan et al.[6] in the *n*-direction, namely RAND, as follows:

$$T_n(x) = \gamma_1 T_{n-1}(x) + \gamma_2 T_{n-2}(x) \tag{8}$$
$$n = 2, 3, \ldots, N-1; \text{ and } x = 0, 1, \ldots, \frac{N}{2} - 1$$

where

$$\gamma_1 = \frac{2x+1-N}{n}\sqrt{\frac{4n^2-1}{N^2-n^2}} \tag{9}$$

$$\gamma_2 = \frac{1-n}{n}\sqrt{\frac{2n+1}{2n-3}}\sqrt{\frac{N^2-(n-1)^2}{N^2-n^2}} \tag{10}$$

The initial values for the RAND are as follows:

$$T_0(x) = \frac{1}{\sqrt{N}} \tag{11}$$

$$T_1(x) = (2x+1-N)\sqrt{\frac{3}{N(N^2-1)}} \tag{12}$$

The DTPCs of the *n*th order for all values of the *x*th index are estimated using the DTPCs values of the previous orders: $n-1$ and $n-2$, as shown in **FIGURE** 1. To compute the DTPCs in the range $n = 0, 1, \ldots, N-1$ and $x = \frac{N}{2}, \frac{N}{2}+1, \ldots, N-1$, the symmetry property is utilized to reduce the computation overload as follows:

$$T_n(N-1-x) = (-1)^n T_n(x) \tag{13}$$

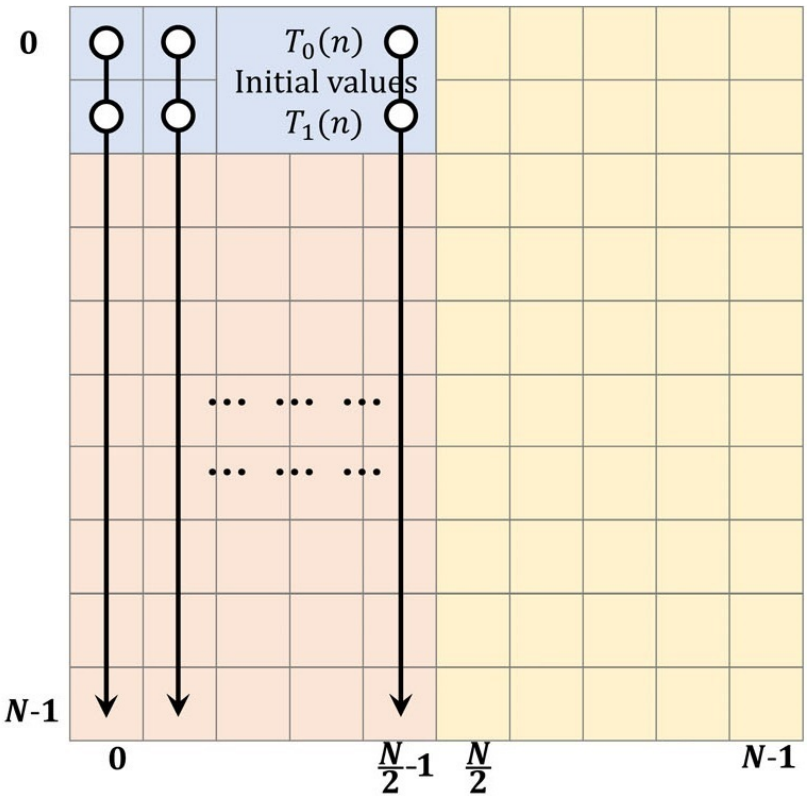

FIGURE 1 The TTRA in the direction of parameter *n*.

This algorithm can generate DTPs for $N < 81$.

3.2 | Recurrence Algorithm in the x-direction (RAXD)

Mukundan et al. in[18] enhanced the performance for computing th DTPCs values by presenting the x-direction recurrence algorithm, namely RAXD, which is given by:

$$T_n(x) = \beta_1 T_n(x-1) + \beta_2 T_n(x-2) \tag{14}$$
$$n = 0, 1, \ldots, N-1; \text{ and } x = 2, 3, \ldots, \frac{N}{2} - 1$$

where

$$\begin{aligned} \beta_1 &= \frac{-n(n+1) - (2x-1)(x-N-1) - x}{x(N-x)} \\ \beta_2 &= \frac{(x-1)(x-N-1)}{x(N-x)} \end{aligned} \tag{15}$$

The initial values for RAXD are given by:

$$\begin{aligned} T_n(0) &= -\sqrt{\frac{N-n}{N+n}}\sqrt{\frac{2n+1}{2n-1}}\, T_{n-1}(0), \\ T_n(1) &= \left(1 + \frac{n(1+n)}{1-N}\right) T_n(0), \end{aligned} \tag{16}$$

where $T_0(0) = \frac{1}{\sqrt{N}}$. The DTPCs values of the xth index for all the nth order are computed using the previous polynomial values: $x-1$ and $x-2$, as shown in **FIGURE** 2. In addition, the symmetry relation in (13) are utilized to compute the rest of the values of the DTPCs. However, the algorithm can generate DTPCs for $N < 1096$.

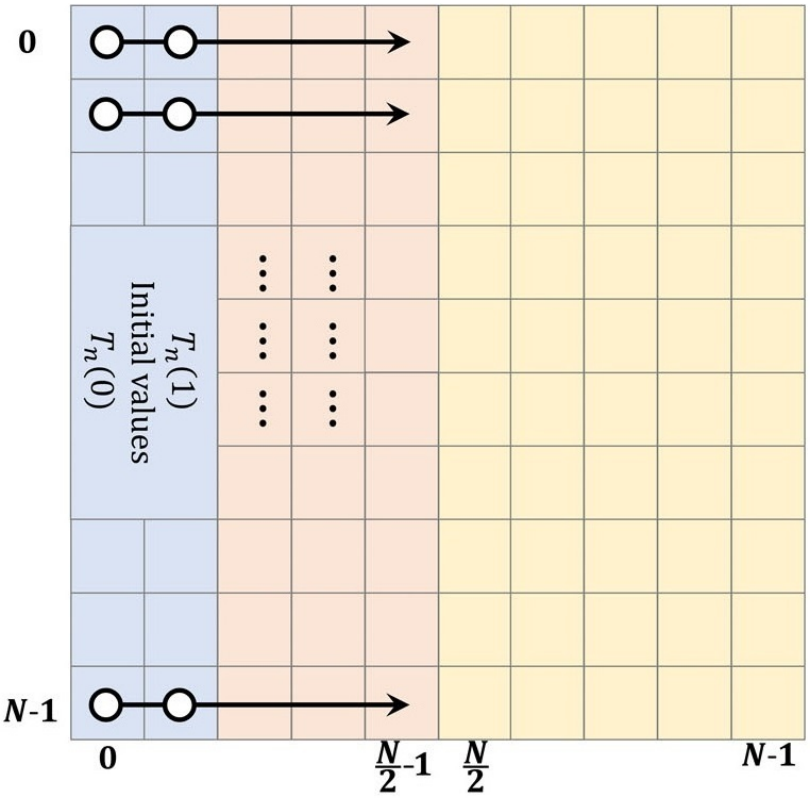

FIGURE 2 The TTRA in the direction of parameter x.

3.3 | Recurrence Algorithm Using Gram-Schmidt (RAGS)

Camacho-Bello and Rivera-Lopez in[20] developed the RAGS and employed the Gram-Schmidt algorithm to enhance the orthogonality of the DTPs. The proposed RAGS is defined as follows:

$$\omega_n T_n(x) = \omega T_{n-1}(x) - \omega_{n-1} T_{n-2}(x) \quad (17)$$
$$n = 0, 1, \dots, N-1; \text{ and } x = 1, 2, \dots, N-1$$

where

$$\omega = 2x - N + 1 \quad (18)$$

$$\omega_n = n\sqrt{\frac{N^2 - n^2}{(2n-1)(2n+1)}} \quad (19)$$

The initial condition used for this algorithm are similar to that in (11). The experimental analysis performed in[20] showed that the performance of the algorithm is slightly better than RAND[6]. On the other hand, its performance are less than the RAXD[18]. To tackle this problem the Gram-Schmidt algorithm was utilized to compensate the error in wavefront expansion[25]. However, this algorithm attains the orthogonality condition, its limitation are: 1) the high computation cost resulted from the implementation of the Gram-Schmit algorithm as well as the computation of the values of the DTPCs for the entire DTPs array (please see (17)), 2) the computed values of the DTPCs using the gram-Schmidt are deviated from the actual values, especially from those of the high order polynomials which affect the computed moments in turn the acquired signal details are deviated from real values.

3.4 | Recurrence Algorithm Using both *n*- and *x*-direction algorithms (RANX)

This algorithm, namely RANX, is presented by Abdulhussain et al. in[19] which integrated both the *n*- and *x*-direction recurrence algorithms. First, this algorithm computed the values of the DTPCs using the *x*-direction recurrence relation for $n = 0, 1, \cdots, \frac{N}{2} - 1$ and $x = 0, 1, \cdots, \frac{N}{2} - 1$. Then, it utilizes the *n*-direction recurrence algorithm in the range $n = \frac{N}{2}, \frac{N}{2} + 1, \cdots, N-1$ and $x = L_x, L_x + 1, \cdots, \frac{N}{2} - 1$, where L_x is computed at the border of an oval shape (see Equation (20))[19]. Thereafter, the values of the DTPCs are computed using backward recurrence of the *x*-direction algorithm in the range $n = \frac{N}{2}, \frac{N}{2} + 1, \cdots, N-1$ and $x = L_x, L_x - 1, \cdots, L_x - 12$. Although this algorithm is fast, the orthogonality condition is destroyed for $N > 4000$.

4 | THE PROPOSED ALGORITHM

The proposed algorithm is designed such that the DTPs satisfy the orthogonality condition as well as low computational cost. The proposed algorithm is designed based on integrating both of the recurrence algorithms in the *n*- and *x*-directions.

In other words, the proposed algorithm is the expansion of RANX, presented in[19]. However, to maintain the values of the DTPCs destroyed as the order of the polynomial increases, an empirical study is performed to investigate the location where the values of the DTPCs fall to zero, i.e. the proposed algorithm will set the location adaptively. For convenience, we refer to the proposed algorithm as Adaptive recurrence algorithm using *n*- and *x*-directions (ARANX).

Assume a DTP is generated with a size of $N \times N$. We utilize the algorithm in[19] to generate the values of the DTPCs without zeroing out the values in the range of $x < L_x - 12$. **FIGURE** 3 shows the DTPCs array (left), DTP basis functions for three different polynomials orders (center) and their corresponding zoom within the region $\pm(L_x - 12)$ (right).

From **FIGURE** 3, it can be observed that the DTP basis functions is stable when the order ($\leq \frac{N}{2}$), i.e. $n \leq 1500$.

On the other hand, when the polynomial order is greater than $\frac{N}{2}$, i.e. $n > 1500$, the DTP basis functions become unstable. More specifically, in this case $n \geq 1600$, the DTP basis functions become unstable (**FIGURE** 3 center top and center middle).

It is also observed that the assumption of zeroing out DTPCs for $x \leq L_x - 12$ is not accurate because the values of the polynomial is greater than 20×10^{-5}; thus, this will lead to distortion when transforming/reconstructing a signal to/from the moment domain. However, selecting $x << (L_x - 12)$ will yield to DTPCs to be unstable.

For more elucidation, **FIGURE** 4 shows the DTPCs for $n = 1800$ and $n = 2100$. It can be noted that the DTPCs are stable beyond the value of $L_x - 12$. For example, at $n = 1800$, the polynomial coefficients are stable for $x \geq 263$ and the polynomial coefficients become unstable for $x = 262 \rightarrow 0$. Thus the stable values of DTPC can be computed for $x > L_x - 37$. On the same basis, the DTPCs values for $n = 2100$ can be computed for $x > L_x - 39$. In addition, **FIGURE** 5 shows the DTPCs for

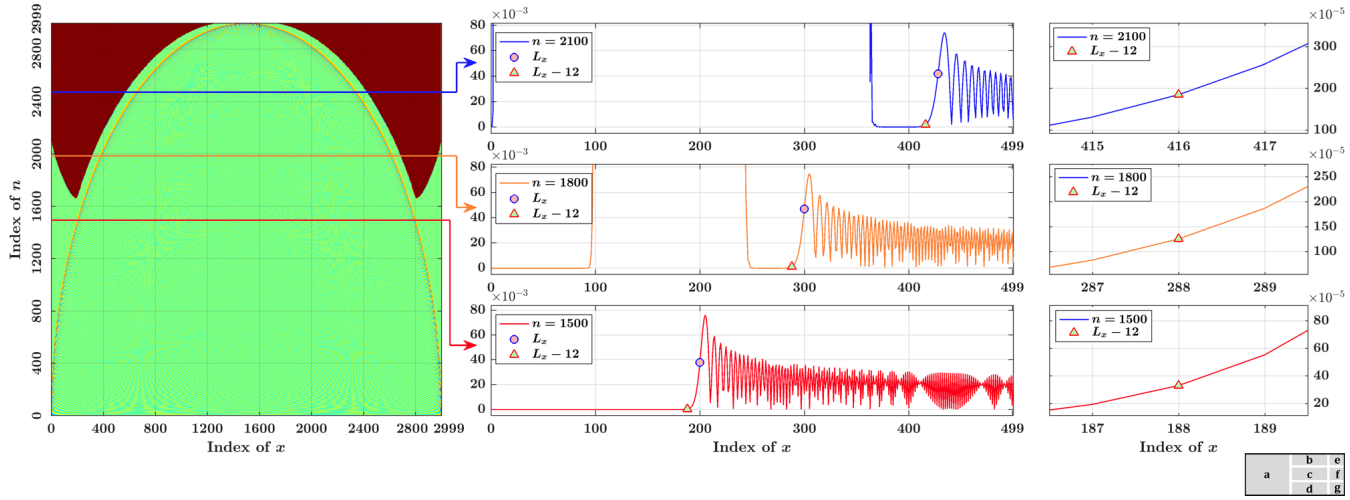

FIGURE 3 DTPC generated using RANX algorithm[19]

$N = 1500$ with two orders $n = 1050$ and $n = 1350$. It can be noted that the DTPCs stable beyond the value of $L_x - 12$. For example, at $n = 1050$, the polynomial coefficients are stable for $x \geq 184$ and the polynomial coefficients become unstable for $x = 183 \rightarrow 0$. Thus the stable values of DTPC can be computed for $x > L_x - 30$. On the same basis, the DTPCs values for $n = 1350$ can be computed for $x > L_x - 44$.

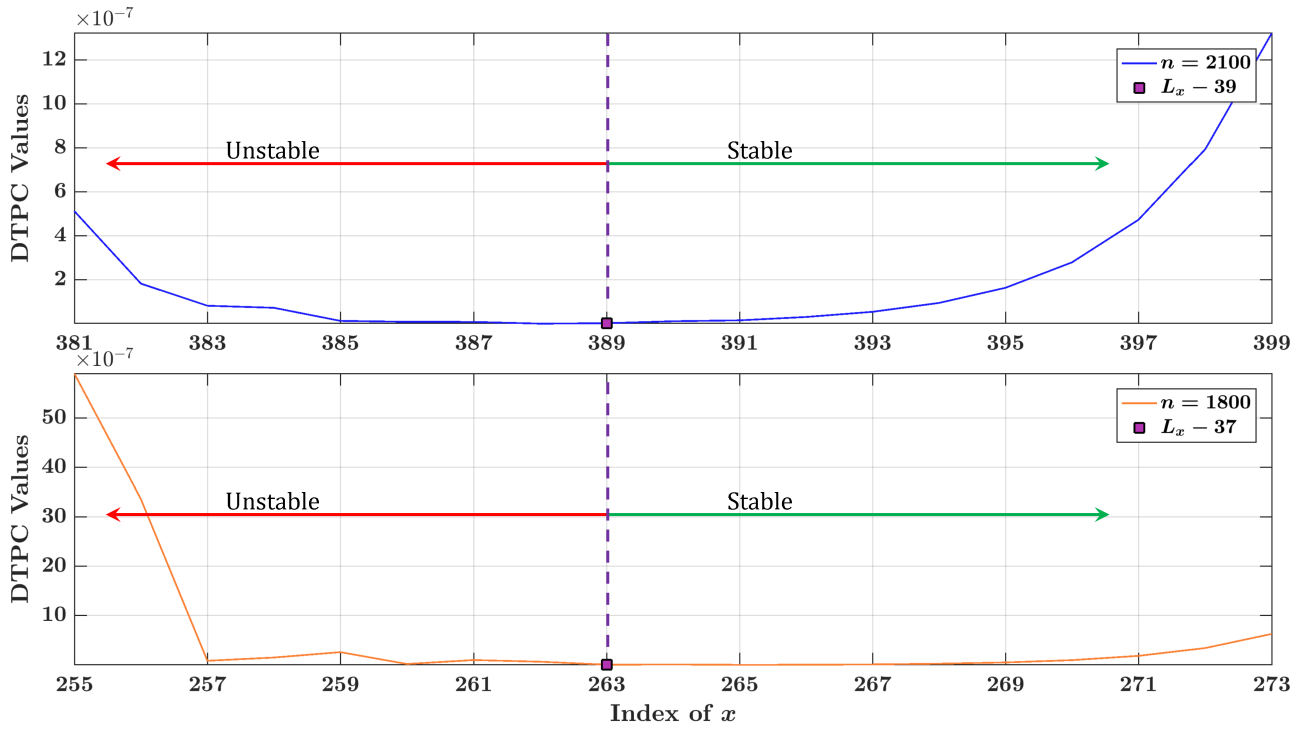

FIGURE 4 DTPC generated using RANX algorithm[19] for $N = 3000$.

From the previous investigation, it can be observed that the optimum values of x to start zeroing out the DTPCs values should be deceptively selected for each polynomial order as well as the polynomial size. To find the optimum value of x, the location where start to zeroing out the polynomial values at for each polynomial order n, we find the location of x where the new DTPC

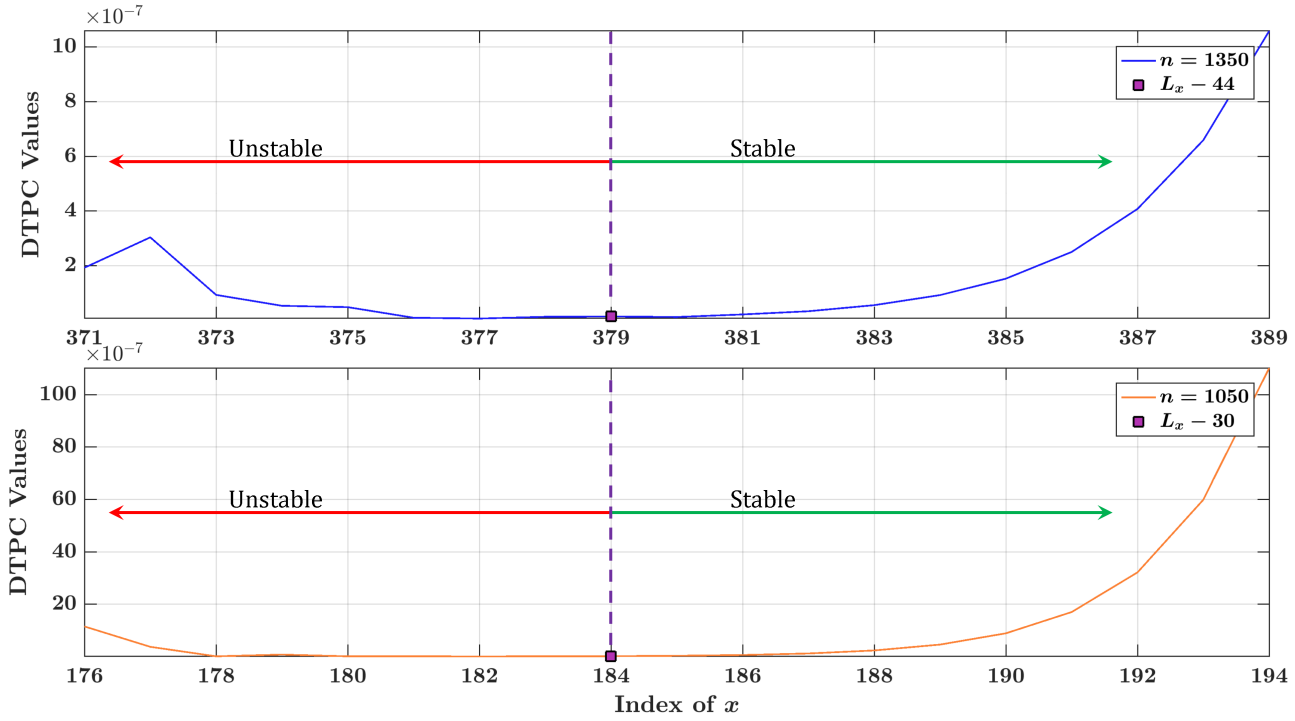

FIGURE 5 DTPC generated using RANX algorithm[19] for $N = 1500$.

value is greater than the previous DTPC value. This will indicate that the DTPC values at that location will start to be unstable; and thus zeroing out all the DTPCs values located in the region $0 < x < L_{x_{optimum}}$.

The algorithm detailed description is as follows:

i. The initial values ($T_n(0)$ and $T_n(1)$) are computed using equation (16) for $1 < n < \frac{N}{2} - 1$. where $T_0(0) = T_0(1) = \frac{1}{\sqrt{N}}$.

ii. The values of the DTPCs in the range $0 < n < \frac{N}{2} - 1$ and $2 < x < \frac{N}{2} - 1$ are computed using the recurrence relation in equation (14).

iii. The values of the DTPCs in the range $\frac{N}{2} < n < N - 1$ and $L_x < x < \frac{N}{2} - 1$ are computed using the recurrence relation in equation (17), where L_x is the boundary of oval shape and is computed as follows:

$$L_x = \frac{N}{2} - \sqrt{\left(\frac{N}{2}\right)^2 - \left(\frac{n}{2}\right)^2} \tag{20}$$

iv. The values of the DTPCs in the range $\frac{N}{2} < n < N - 1$ and $L_{x_{optimum}} \leq x < L_x$ are computed using the recurrence relation in equation (14) in backward manner. The value of $L_{x_{optimum}}$ is found such that each newly computed value of $T_n(x)$ is compared with its previous value $T_{n+1}(x)$. When $T_n(x) < T_{n+1}(x)$ the recurrence relation continues to compute the next values,$T_{n-1}(x)$; else the algorithm stops and consider the previous value is optimum and set the rest of the DTPCs value for the current order (n) to zero (DTPCs values are zeroed in the range $0 < x < L_{x_{optimum}}$).

v. The DTPCs values in the range $n = 0, 1, \ldots, N - 1$ and $x = \frac{N}{2}, \frac{N}{2} + 1, \ldots, N - 1$ (second half of the array) is computed symmetry relation defined in Equation (13).

The steps of the proposed algorithm are shown in **FIGURE** 6. For more clarification, Algorithm 1 illustrates the proposed algorithm (ARANX) with an input of size N and maximum order Ord.

Algorithm 1 Generation of Tchebichef Polynomial

Input: N, Ord

N is the polynomial size,

Ord is the maximum polynomial order.

Output: $T_n(x)$

$T_0(0) \leftarrow \frac{1}{\sqrt{N}}$

$T_0(1) \leftarrow \frac{1}{\sqrt{N}}$

for $n = 1 : \min\left\{Ord - 1, \frac{N}{2} - 1\right\}$ **do**

  $T_n(0) \leftarrow -\sqrt{\frac{N-n}{N+n}}\sqrt{\frac{2n+1}{2n-1}}\,T_{n-1}(0)$

  $T_n(1) \leftarrow \left(1 + \frac{n(1+n)}{1-N}\right) T_n(0)$

end for

▷ Compute DTPCs for first quarter using x-direction

for $x = 2 : \frac{N}{2} - 1$ **do**

  $\beta_2 \leftarrow \frac{(x-1)(x-N-1)}{x(N-x)}$

  for $n = 0 : \min\left\{Ord - 1, \frac{N}{2} - 1\right\}$ **do**

    $\beta_1 \leftarrow \frac{-n(n+1)-(2x-1)(x-N-1)-x}{x(N-x)}$

    $T_n(x) \leftarrow \beta_1 T_n(x-1) + \beta_2 T_n(x-2)$

  end for

end for

for $n = \frac{N}{2} : Ord$ **do**

▷ Compute DTPCs for second quarter using n-direction

  $L_x \leftarrow \frac{N}{2} - \sqrt{\left(\frac{N}{2}\right)^2 - \left(\frac{n}{2}\right)^2}$

  for $x = L_x : \frac{N}{2} - 1$ **do**

    $\gamma_1 \leftarrow \frac{2x+1-N}{n}\sqrt{\frac{4n^2-1}{N^2-n^2}}$

    $\gamma_2 \leftarrow \frac{1-n}{n}\sqrt{\frac{2n+1}{2n-3}}\sqrt{\frac{N^2-(n-1)^2}{N^2-n^2}}$

    $T_n(x) \leftarrow \gamma_1 T_{n-1}(x) + \gamma_2 T_{n-2}(x)$

  end for

end for

for $n = \frac{N}{2} : Ord$ **do**

▷ Compute DTPCs for second quarter using x-direction backwardly

  $L_x \leftarrow \frac{N}{2} - \sqrt{\left(\frac{N}{2}\right)^2 - \left(\frac{n}{2}\right)^2}$

  for $x = L_x + 1 : -1 : 2$ **do**

    $\beta_2 \leftarrow \frac{(x-1)(x-N-1)}{x(N-x)}$

    $\beta_1 \leftarrow \frac{-n(n+1)-(2x-1)(x-N-1)-x}{x(N-x)}$

    $T_n(x-2) \leftarrow -\frac{\beta_1}{\beta_2}T_n(x-1) + \frac{1}{\beta_2}T_n(x)$

    if $T_n(x-2) > T_n(x-1)$ **then**

      $T_n(x-2) \leftarrow 0$

      $L_{x_{optimum}} = x - 1$

      Break

    end if

  end for

end for

for $n = 0 : N - 1$ **do**

▷ Compute DTPCs for second half using symmetry condition

  for $x = \frac{N}{2} : N - 1$ **do**

    $T_n(N-1-x) \leftarrow (-1)^n\, T_n(x)$

  end for

end for

5 | EXPERIMENTAL RESULTS

This section presents the performance evaluation of the proposed recurrence algorithm in terms of the computational cost, signal reconstruction, and a comparison with state-of-the-art algorithms.

5.1 | Preservation of Orthogonality Condition

To preserve that the moments (descriptor) is linearly independent and there are no redundancy in the information, the orthogonality condition should be preserved[20]. The orthogonality condition defined in equation (3) can be written in matrix form as follows:

$$\hat{\mathbb{I}} = \mathbf{T} \times \mathbf{T}' \tag{21}$$

where $\hat{\mathbb{I}}$ represents the identity matrix, and $(\boldsymbol{T})$ represents the matrix form the of the DTP ($T_n(x)$). The universal similarity index (UQI) presented in[26] is used to estimate the structural similarity index between the identity matrix with that of the DTP. Let $\mathbb{I}$ be a matrix of size $N \times N$, then UQI is given as[20]:

$$UQI = \frac{4\sigma_{kp}\mu_k\mu_p}{(\mu_k^2 + \mu_p^2)(\sigma_k^2 - \sigma_p^2)} \tag{22}$$

where σ_k and σ_p are the standard deviation for the matrix $\mathbb{I}_{i,j}$ and the matrix $\hat{\mathbb{I}}_{i,j}$, respectively. In addition, μ_k and μ_p are the mean value for the matrix $\mathbb{I}_{i,j}$ and the matrix $\hat{\mathbb{I}}_{i,j}$, respectively. The value σ_{kp} is computed as follows:

$$\sigma_{kp} = \frac{1}{N^2 - 1} \sum_{i=0}^{N-1} \sum_{j=0}^{N-1} \left[\mathbb{I}_{i,j} - \mu_k\right] \left[\hat{\mathbb{I}}_{i,j} - \mu_p\right] \tag{23}$$

Similar implementation of orthogonality test condition of moment kernel presented by[20] (Algorithm 2) is utilized in this paper.

Algorithm 2 Orthogonality Test[20]

1: $Error \leftarrow 0.99999$
2: **for** $N = 0$ to H **do**
3: $\quad UQI \leftarrow 1$
4: $\quad n \leftarrow 1$
5: $\quad \mathbf{T} = \left\{T_n(x)\right\}_{i,j=0}^{i,j=N-1}$
6: $\quad$ **while** $UQI > Error$ and $n < N$ **do**
7: $\quad\quad n \leftarrow n + 1$
8: $\quad\quad \hat{\mathbb{I}} \leftarrow \mathbf{T}_{i,j} \times \mathbf{T}'_{i,j}$ for $i = 0, 1, \ldots, N-1$ and $j = 0, 1, \ldots, n$
9: $\quad\quad UQI \leftarrow \frac{4\sigma_{kp}\mu_k\mu_p}{(\mu_k^2+\mu_p^2)(\sigma_k^2-\sigma_p^2)}$
10: $\quad$ **end while**
11: $\quad q_N \leftarrow n$
12: **end for**

Algorithm 2 is utilized to test the orthogonality condition of the algorithms: 1) DTP using RAXD[18], 2) DTP using RAGS[20], 3) DTP using RANX[19], and 4) the proposed algorithm. It is noteworthy to mention that when q_N is a straight line ($q_N = N$), the orthogonality test of the DTP is correct. **FIGURE** 7 illustrated the obtained values of q_N for the aforementioned recurrence algorithms. Moreover, it can be noted that the proposed algorithm (ARANX) and RAGS preserves the orthogonality condition. In addition, **TABLE** 1 lists the maximum value q_N that satisfy the orthogonality condition for different resolutions. From the **TABLE** 1, it is can be observed that the Gram-Schmidt and the proposed algorithms outperforms other algorithms in terms of maximum size that can be generated as well as preserving the orthogonality condition.

TABLE 1 The maximum value of q_N that satisfy the orthogonality condition

	Algorithms			
Resolution $N \times N$	RAXD x-direction [18]	RANX [19]	RAGS x-direction [20]	ARANX Proposed
1280×1280	1267	642	1280	1280
1600×1600	1407	804	1600	1600
2048×2048	1630	1028	2048	2048
2560×2560	1849	1284	2560	2560
3000×3000	2020	1505	3000	3000
3264×3264	2114	1638	3264	3264

5.2 | Algorithms Reconstruction Ability

The proposed method is evaluated in terms of reconstruction ability using sinusoidal Siemens star (SSS) which is utilized to test the optical systems resolution. The SSS consists of sinusoidal oscillations in a polar coordinate system such that the spatial frequency varies for concentric circles of different sizes. The SSS pattern is given by [27]:

$$I(\theta) = a + b\sin(\omega\theta - \phi) \tag{24}$$

where I represents the image intensity, θ the polar angle for the sinusoidal function, a is the mean intensity value, b represents the amplitude of the intensity oscillation, ω depicts the number of cycles, and ϕ is the offset of the potential phase. In the experiment, two test images are utilized with the following parameters: $a = 0$, $b = 255$, $\phi = 0$, and $\omega = 200$, and 400. Note that the size of the images used are 4000×4000 with $\omega = 200$ and 4000×8000 with $\omega = 400$. The original test images are shown in **FIGURE** 8.

The images shown in **FIGURE** 8 are first transformed into moment domain by specific moment order (please see Equation (6)) and reconstructed back to obtain ($\hat{I}$). After obtaining the reconstructed image, the normalized mean square error is computed as follows:

$$NMSE = \frac{\sum_{x\in X}\sum_{y\in Y}\left(I - \hat{I}\right)^2}{\sum_{x\in X}\sum_{y\in Y}(I)^2} \tag{25}$$

The obtained results are shown in **FIGURE** 9. It can be observed from the results that the proposed algorithm and Gram-Schmidt algorithm can reconstruct the image perfectly with a $NMSE$ values of zero and maximum moment order. on the other hand, RANX [19] shows an error when reconstructing the image for image size of 4000×4000 because of the approximation used in their algorithm which lead to slight propagation error in the DTPCs. While for image size of 8000×8000, RANX [19] unable to reconstruct the image because of the high propagation error and instability of DTPCs' values. For RAXD [18], the algorithm unable to reconstruct the image for both image size of 4000×4000 and 8000×8000 due to the instability of DTPCs' values which occurs in the polynomial generation process.

5.3 | Computation Cost Analysis

The evaluation of the computation cost is based on time required to generate the DTP with a size of N and order n. Note that the maximum order of DTP is equal to the size of the polynomial, i.e. N.

The recurrence relations RAND [6] and RAXD [18] compute only 50% of the coefficients and the rest are computed using the similarity relation. While RAGS [20] computed 100% of the coefficients. RANX [19] computes less than 50% of the coefficients. On the other hand, the number of DTPCs computed by the proposed algorithm is slightly greater than RANX and less than 50%. Note that RAXD, RANX, and ARANX utilize the similarity relation to compute the rest of the DTP coefficients.

FIGURE 10 shows the computation time of DTPCs. Obviously, the time required for RAGS is very large compared to other algorithms. For example, the time required to compute a polynomial with order 100 and size of 1000 is 0.06 seconds compared

with ~ 0.004 for the ARANX, RANX, and RAXD algorithms. In other words, the improvement of ARANX is $\sim 93\%$. Moreover, for polynomial order of 200 and size of 8000, the computation time of the proposed algorithm is ~ 0.07 seconds, while for RAGS is ~ 2.6 seconds, i.e. the improvement of ARANX is ~ 97 %. The large computation time of RAGS is due to the nested loop used in the algorithm, Gram-Schmidt algorithm, which leads to a dramatic increase in the computation time required to generate the DTPCs.

For more illustration, the improvement in terms of computation time (ICT) is compared between ARANX and RAGS as shown in **FIGURE** 11. Note that ICT is computed as follows[20]:

$$ICT\% = \frac{Time_{GS-DTP} - Time_{ANX-DTP}}{Time_{GS-DTP}} \times 100 \tag{26}$$

It can be observed that the improvement is greater than 90% when the polynomial order larger than 100 for different polynomial sizes. In addition, the improvement is larger than 60% for polynomial orders less than 100.

6 | CONCLUSION

In this paper, a recurrence algorithm is designed to compute the DTPCs. The recurrence algorithm is designed by combining two well-known recurrence algorithms: the n-direction and x-directions recurrence algorithms. In addition, an adaptive threshold is used to stabilize the generation of the DTPCs. The proposed algorithm (ARANX) can generate the DTPCs for high order and large signal size. In addition, the designed algorithm has low computation cost compared to RAGS which is able to generate DTP with high order for large signal size. A comparison is performed between ARANX and the state-of-the-art algorithms to show the promising feature and superior capability of the proposed algorithm computational cost. Moreover, the designed algorithm, ARANX, achieves a better results in terms of signal reconstruction for high polynomial orders.

References

1. Zhou J, Shu H, Zhu H, Toumoulin C, Luo L. Image Analysis by Discrete Orthogonal Hahn Moments. In: Kamel M, Campilho A., eds. *Image Analysis and Recognition*Springer Berlin Heidelberg; 2005; Berlin, Heidelberg: 524–531.

2. Zhu H, Liu M, Shu H, Zhang H, Luo L. General form for obtaining discrete orthogonal moments. *IET Image Processing* 2010; 4(5): 335.

3. Yap PT, Paramesran R, Ong SH. Image Analysis Using Hahn Moments. *IEEE Transactions on Pattern Analysis and Machine Intelligence* 2007; 29(11): 2057–2062.

4. Mahmmod BM, Abdul-Hadi AM, Abdulhussain SH, Hussien A. On Computational Aspects of Krawtchouk Polynomials for High Orders. *Journal of Imaging* 2020; 6(8): 81. doi: 10.3390/jimaging6080081

5. Abdul-Hadi AM, Abdulhussain SH, Mahmmod BM. On the computational aspects of Charlier polynomials. *Cogent Engineering* 2020; 7(1). doi: 10.1080/23311916.2020.1763553

6. Mukundan R, Ong S, Lee P. Image analysis by Tchebichef moments. *IEEE Transactions on Image Processing* 2001; 10(9): 1357–1364.

7. Abdulhussain SH, Ramli AR, Mahmmod BM, Saripan MI, Al-Haddad S, Jassim WA. A New Hybrid form of Krawtchouk and Tchebichef Polynomials: Design and Application. *Journal of Mathematical Imaging and Vision* 2018: 1–16.

8. Senapati RK, Pati UC, Mahapatra KK. Reduced memory, low complexity embedded image compression algorithm using hierarchical listless discrete Tchebichef transform. *IET Image Processing* 2014; 8(4): 213.

9. Rahmalan H, Ernawan F, Abu NA. Tchebichef Moment Transform for colour image dithering. In: . 2. IEEE. ; 2012: 866–871.

10. Abdulhussain SH, Rahman Ramli A, Mahmmod BM, et al. A Fast Feature Extraction Algorithm for Image and Video Processing. In: IEEE; 2019: 1–8

11. Mahmmod BM, Ramli bAR, Abdulhussain SH, Al-Haddad SAR, Jassim WA. Signal compression and enhancement using a new orthogonal-polynomial-based discrete transform. *IET Signal Processing* 2018; 12(1): 129–142.

12. Mahmmod BM, Ramli AR, Baker T, Al-Obeidat F, Abdulhussain SH, Jassim WA. Speech Enhancement Algorithm Based on Super-Gaussian Modeling and Orthogonal Polynomials. *IEEE Access* 2019; 7: 103485–103504.

13. Monge-Álvarez J, Hoyos-Barceló C, Dahal K, Higuera C.-d.-lP. Audio-cough event detection based on moment theory. *Applied Acoustics* 2018; 135: 124–135.

14. Radeaf HS, Mahmmod BM, Abdulhussain SH, Al-Jumaeily D. A steganography based on orthogonal moments. In: ICICT '19. ACM Press; 2019; New York, New York, USA: 147–153.

15. Xiao B, Lu G, Zhang Y, Li W, Wang G. Lossless image compression based on integer Discrete Tchebichef Transform. *Neurocomputing* 2016; 214: 587–593.

16. Oliveira PA, Cintra RJ, Bayer FM, Kulasekera S, Madanayake A. A discrete Tchebichef transform approximation for image and video coding. *IEEE Signal Processing Letters* 2015; 22(8): 1137–1141.

17. Oliveira PA, Cintra RJ, Bayer FM, Kulasekera S, Madanayake A. Low-complexity image and video coding based on an approximate discrete Tchebichef transform. *IEEE transactions on circuits and systems for video technology* 2016; 27(5): 1066–1076.

18. Mukundan R. Some Computational Aspects of Discrete Orthonormal Moments. *IEEE Transactions on Image Processing* 2004; 13(8): 1055–1059.

19. Abdulhussain SH, Ramli AR, Al-Haddad SAR, Mahmmod BM, Jassim WA. On Computational Aspects of Tchebichef Polynomials for Higher Polynomial Order. *IEEE Access* 2017; 5(1): 2470–2478.

20. Camacho-Bello C, Rivera-Lopez JS. Some computational aspects of Tchebichef moments for higher orders. *Pattern Recognition Letters* 2018; 112: 332–339.

21. Foncannon JJ. Irresistible integrals: symbolics, analysis and experiments in the evaluation of integrals. *The Mathematical Intelligencer* 2006; 28(3): 65–68.

22. Jan F, Tomáš S, Barbara Z. *Moments and Moment Invariants in Pattern Recognition* . 2009.

23. Thung KH, Paramesran R, Lim CL. Content-based image quality metric using similarity measure of moment vectors. *Pattern Recognition* 2012; 45(6): 2193–2204.

24. Mizel AKE. Orthogonal Functions Solving Linear functional Differential EquationsUsing Chebyshev Polynomial. *Baghdad Science Journal* 2008; 5(1): 143–148.

25. Malacara D. *Optical shop testing*. John Wiley & Sons . 2007.

26. Wang Z, Bovik AC. A universal image quality index. *IEEE signal processing letters* 2002; 9(3): 81–84.

27. Birch GC, Griffin JC. Sinusoidal Siemens star spatial frequency response measurement errors due to misidentified target centers. *Optical Engineering* 2015; 54(7): 074104.

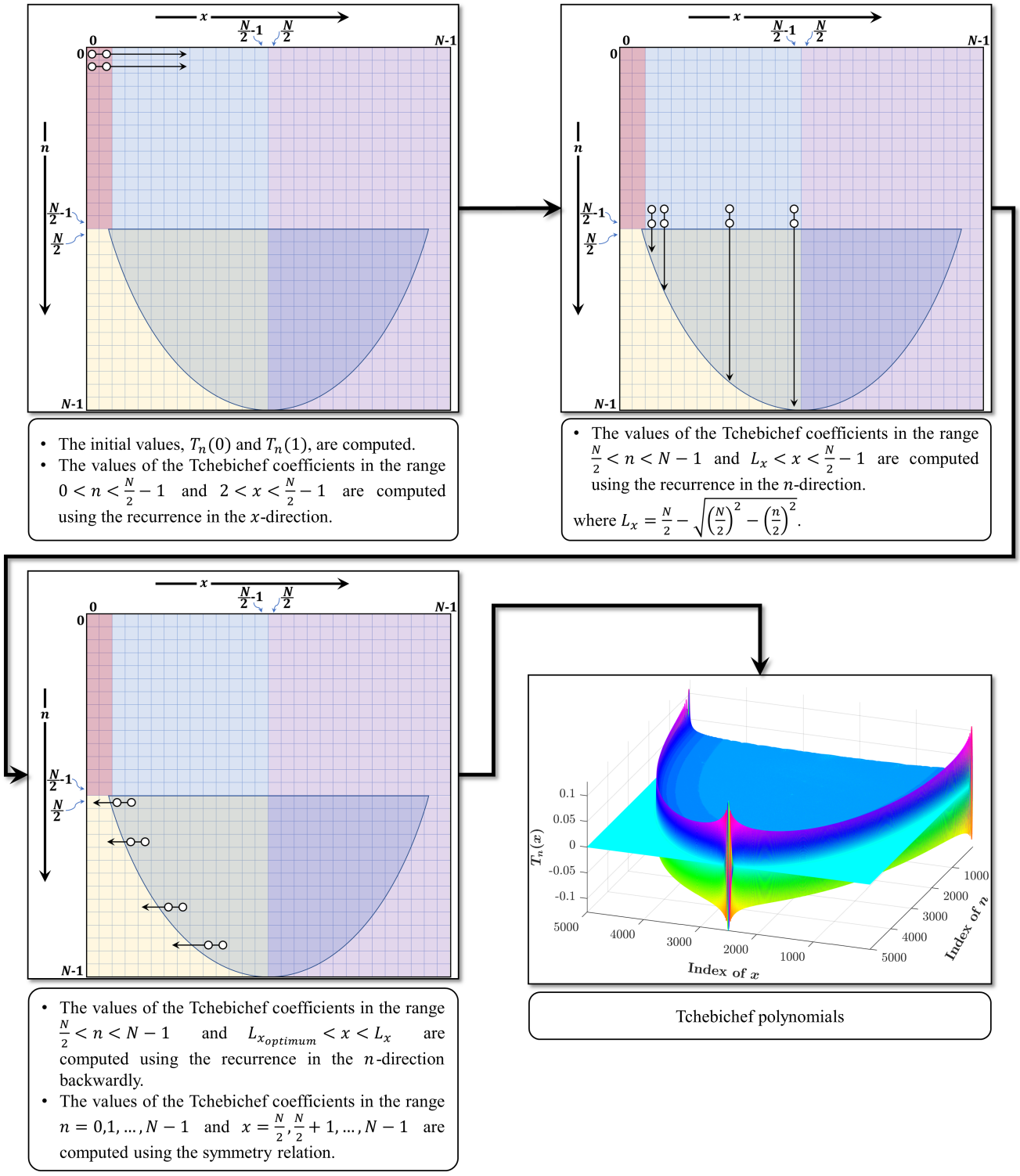

FIGURE 6 The steps of the proposed algorithm.

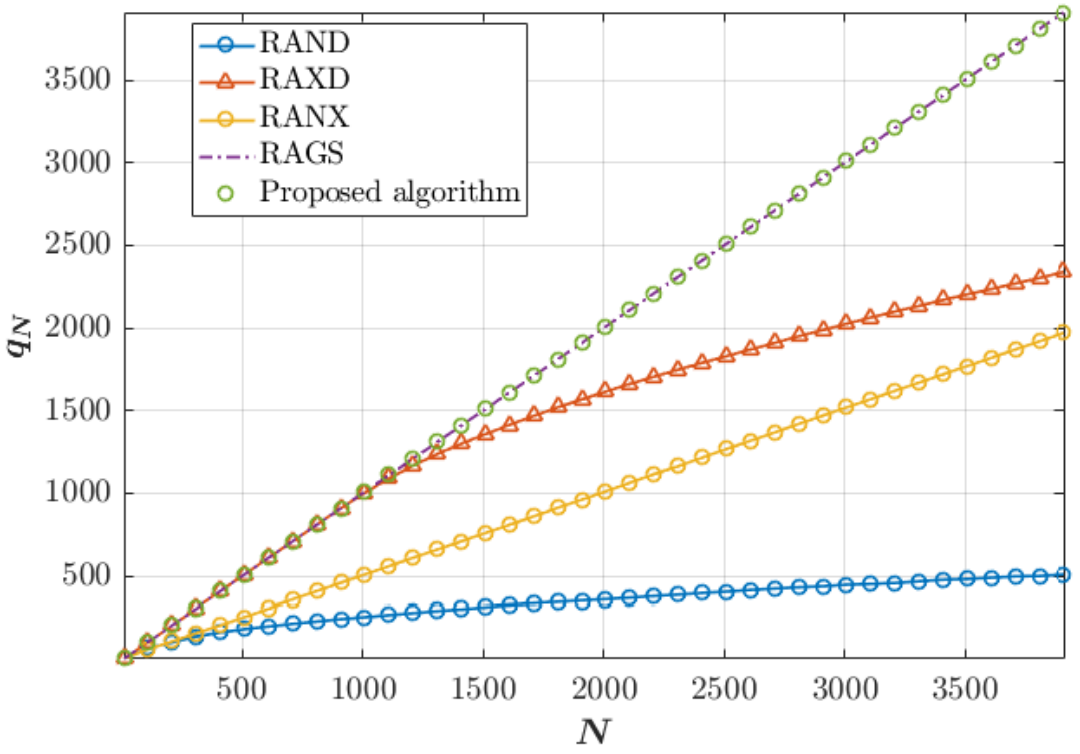

FIGURE 7 Test of the orthogonality condition for different recurrence algorithms

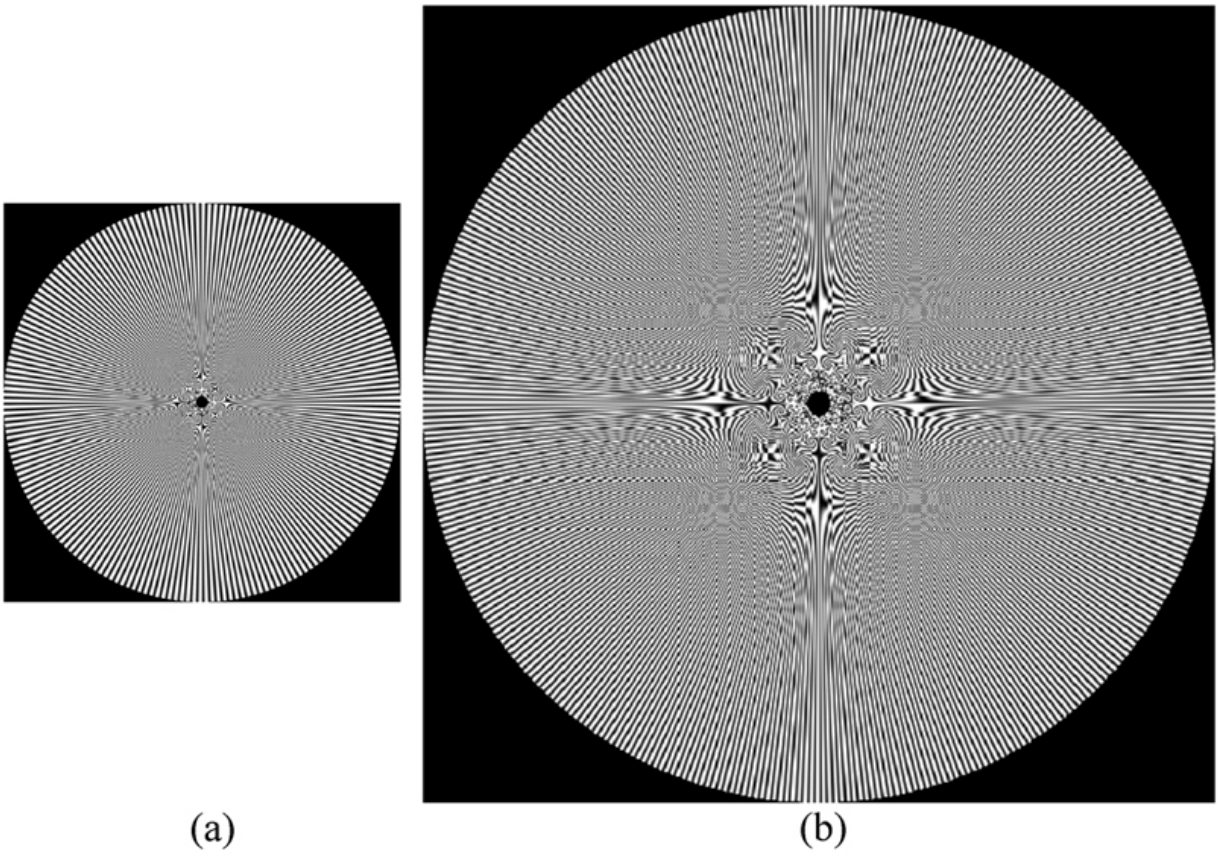

FIGURE 8 Test images used in the experiment (a) 4000×4000 with $\omega = 200$, and (b) 8000×8000 with $\omega = 400$

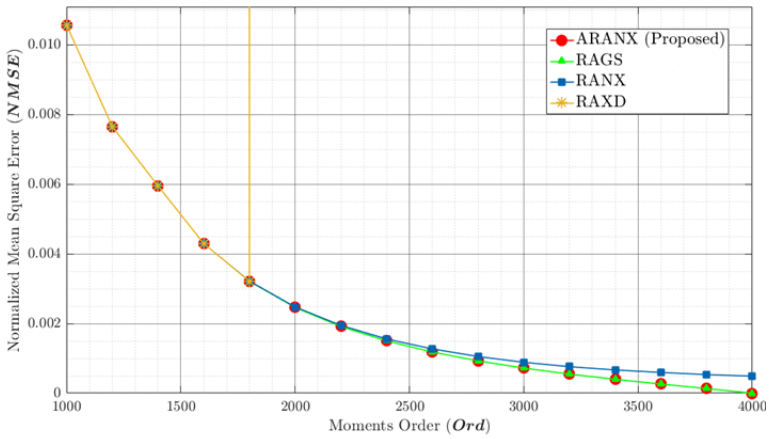

(a)

Algorithm / Order	Order = 500	Order = 1000	Order = 2000	Order = 4000
Proposed				
Gram-Schmidt [20]				
Abdulhussain et al. [19]				
Mukundadn [9]				

(b)

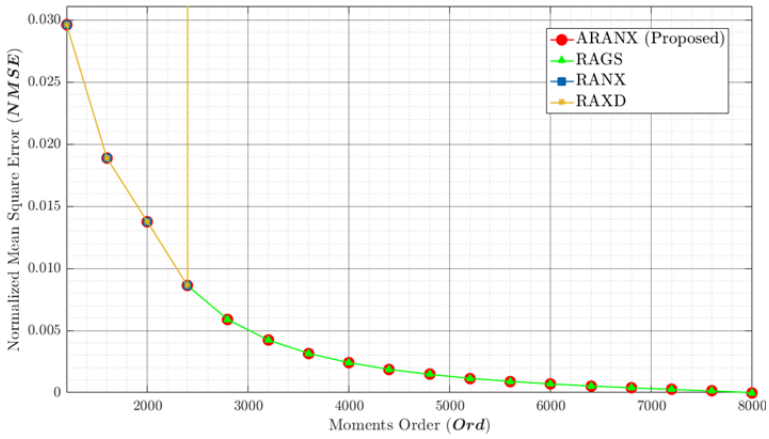

(c)

Algorithm / Order	Order = 1000	Order = 2000	Order = 4000	Order = 8000
Proposed				
Gram-Schmidt [20]				
Abdulhussain et al. [19]				
Mukundadn [9]				

(d)

FIGURE 9 The NMSE and the reconstructed images for different values of order (a) and (b) $NMSE$ and reconstructed images for test image shown in **FIGURE** 8a, (c) and (d) $NMSE$ and reconstructed images for test image shown in **FIGURE** 8b

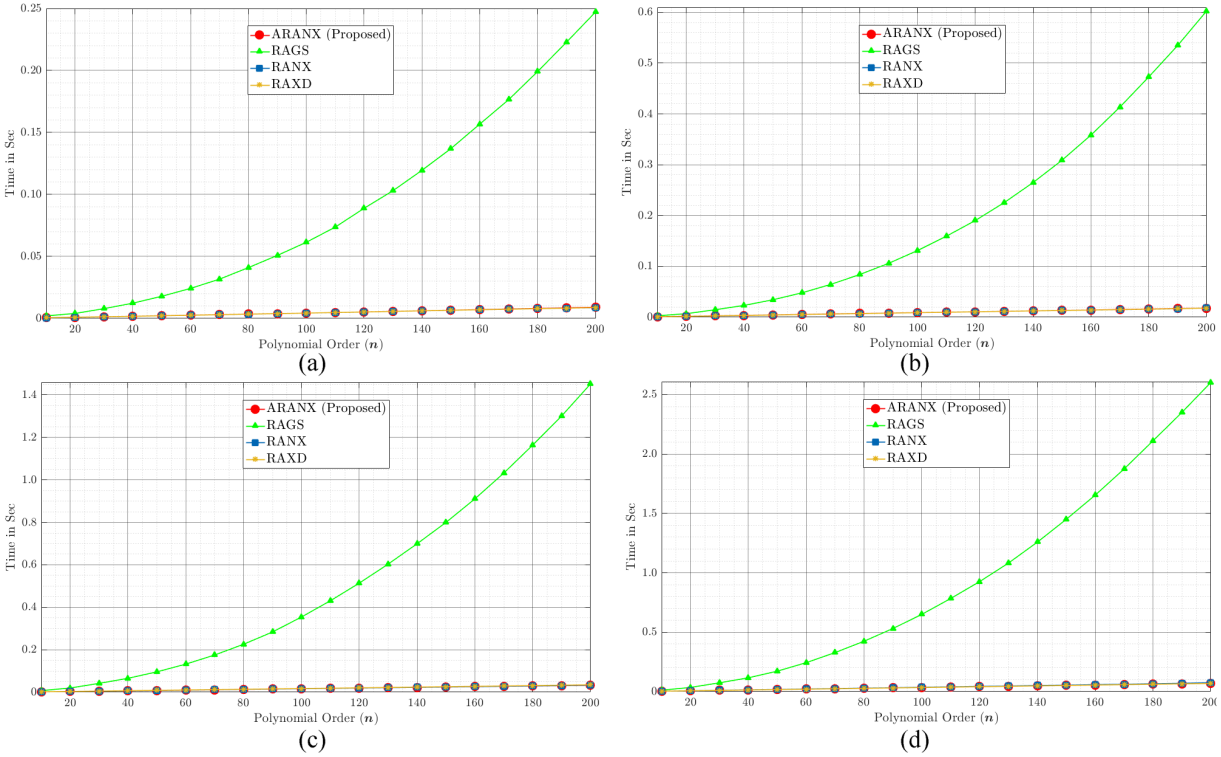

FIGURE 10 The Computation time of the proposed and state-of-the-art algorithms with maximum polynomial order of 200 and signal size of (a) 1000, (b) 2000, (c) 4000, and (d) 8000

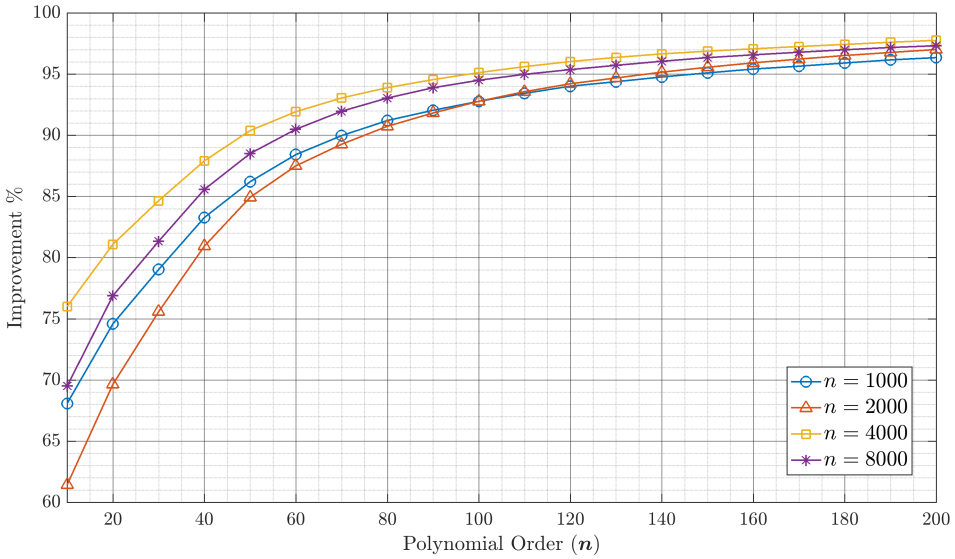

FIGURE 11 The improvement of the proposed algorithm in terms of computation time compared with Gram-Schmidt algorithm